International Journal of Membrane Science and Technology, 2023, Vol. 10, No. 4, pp 2538-2548

Molecular Docking, Dynamics Simulation, And in Silico DFT Studies Of Bromo [1,4] Benzodiazepine Derivatives Are Efficient Ways to Prevent Skin Cancer

B. Brindha[1*], Dr. R. Girija[2]

[1*]Department of chemistry, Queen Mary's College,
[2]Bioinformatics infrastructure facility center, Queen Mary's College, Chennai-04.
Email: brindha2886@gmail.com.

***Corresponding Author:** B. Brindha
*Department of chemistry, Queen Mary's College, [3]Bioinformatics infrastructure facility centre, Queen Mary's college. Email: brindha2886@gmail.com.

Abstract:
Studies have revealed that the most common kind of cancer in the world is skin cancer. Unrepaired deoxyribonucleic acid (DNA) in skin cells can cause genetic abnormalities or mutations that lead to skin cancer. Early detection is crucial because skin cancer is more treatable in its early stages and tends to gradually spread to other areas of the body. Early detection of signs of skin cancer is essential due to the high mortality, increasing morbidity and expensive medical care of the disease. The present study used ligand and structure-based analysis to calculate the interaction between bromo [1,4] benzodiazepine derivatives and 4,5 Diaryl Isoxazole Hsp90 Chaperone Inhibitors: Potential Therapeutic Agents for Cancer. Qikprop revealed that the structures of several antiviral drugs were identical to those of bromo[1,4] benzodiazepine derivatives (1a-1j). bromo [1,4] benzodiazepine derivatives were employed in an in silicodocking experiment, DFT calculations and simulation techniques on skin cancer with PDB ID 2VCI, using Schrodinger Maestro 12.4. Each ligand's interaction was studied, and the potential imperative energy was calculated. In summary, a high potency against skin cancer as observed for the derivative of bromo [1,4] benzodiazepine derivatives with the best binding energy.

Keywords: Skin cancer, Bromo [1,4] benzodiazepine, Molecular Docking, DFT, 2VCI

1. INTRODUCTION

In the current decade, skin cancer is the fifth most frequent type of cancer and one of the deadliest. [1,2,3,4]. Skin cancer is the most prevalent kind of cancer among humans, which is understandable given that the skin is the body's biggest organ. [13]. Nonmelanoma skin cancer (NMSC) and melanoma are the two main categories for skin cancer. Due to underreporting and a lack of diagnostic criteria, it is difficult to pinpoint the precise incidence of skin cancer. Over the past several decades, however, a number of epidemiologic studies have indicated an increase in the incidence of both melanoma and NMSC. [5,6]. 1.198 million persons were affected by non-melanoma skin cancer in 2020, which was the sixth most prevalent kind of cancer and accounted for 6.2% of all cancer cases [7, 8].
A significant family of heterocyclic chemicals, [1,4] benzodiazepines are utilized therapeutically to treat a wide range of human illnesses. The distinct structure of [1,4] benzodiazepines is modelled after a peptide bond. Medicinal chemists' interest in [1,4] benzodiazepines was entirely changed by this intriguing result, from CNS acting medicines to anticancer compounds. [12] Over the past few decades, benzodiazepines have been linked to a number of findings in the literature that emphasize their anticancer activities. The PubChem database contains information on around 35 million compounds. It was made with two Docking apps from the Maestro 12.4 Schrodinger Glide software. Highlight the binding with either an extreme precision (XP) or standard precision (SP) Glide. Strong interactions, sufficient effectiveness against the therapeutic target, and suitable ADMET qualities at a therapeutic dosage are characteristics of a high-quality pharmacological candidate [9]. Computational methods like drug-likeness prediction, in silico ADMET analysis, molecular docking, and molecular dynamics simulations are useful for this since they help find possible pharmaceuticals or compounds from different databases and cut down on the time and expense of experiments involved in drug discovery [10]. Molecular docking has demonstrated efficacy in predicting the binding energy and mechanism of protein-ligand complexes [11], whereas ADMET prediction is a useful tool for assessing a powerful molecule's absorption, distribution, metabolism, excretion, and toxicity [9]. The analysis of these studies will determine the effectiveness of the benzodiazepine derivatives against skin cancer.

2. Materials and methods:

Chemdraw's structural format (SDF) program was used to build the chemical structure. Bonding analysis and simulation studies were performed using Schrödinger's SP, XP, and MGBSA Prime tools.

2.1 Protein preparation:
The RCSB Protein Data Bank (PDB) website provides the X-ray crystal structure and coordinate file for the human phosphodiesterase type 5 (2VCI) protein domain in relation to sildenafil [19]. The retrieved protein was edited using Swiss-PDB Viewer 4.1.0 to add missing residues, rectify mismatched bonds, and correct side chain abnormalities. After giving to the file the name Target. pdb, it was stored for further research.

2.2 Preparation of Ligands:
Ligand structures were drawn, stored in SDF format, and then imported by choosing the file. The imported ligands (1a-1j) were configured to minimize using the force field OPLS3e. All bromo [1,4] benzodiazepine derivative structures underwent minimization computations.

2.3 Docking Study:
Molecular docking is a vital technique in structural molecular biology and computer-assisted drug development. Predicting the dominant binding mode(s) of a ligand with a protein that has a known three-dimensional structure is the aim of ligand-protein docking. Effective docking systems need a scoring system that appropriately evaluates candidate dockings and efficiently explores high-dimensional areas. Lead optimization greatly benefits from the use of docking to do virtual screening on huge chemical libraries, score the findings, and offer structural suggestions for how the ligands block the target. [14]. Research on the ligand-binding site, ligand orientation, and molecular interactions between proteins and ligands has frequently used this approach [15]. The technique is occasionally used in the calculation of protein-ligand binding affinity since scoring systems for molecular docking simulation are frequently developed based on thermodynamic energy terms in protein-ligand binding [16,17,18].

2.4 Evaluation of ADME characteristics:
In the early stages of drug research and development, pharmacological profile evaluation is a crucial duty. The Schrodinger QikProp program was used to calculate the ADME characteristics and screen the compounds. The proportion of oral absorption by humans (QPPMDCK), water solubility (QPlogS), partition coefficient (QP log P octanol/water), and apparent MDCK permeability (QPPMDCK). The prediction of molecular weight, hydrogen bond donors and acceptors, and blood-brain barrier permeability (QPlogBB) are among the critical features used for ligand screening [20,21]. A viable oral medication must satisfy certain guidelines in order to be approved: its molecular weight must be between 515 and 762 Da, log P must be 7 or less, and it must have between 0 and 5 H-bond donors and 1 to 7 H-bond acceptors, according to research [22].

Title	mol MW	donorHB	acceptHB	QPlogPo/w	QPlogS	QPPCaco	QPlogBB	QPPMDCK	QPlogKp	#metab	QPlogKhsa	Human Oral Absorption	Percent Human Oral Absorption	PSA	Rule Of Five	CNS	#rtvFG
1A	515.084	1	2.5	5.58	-5.629	1464.959	0.921	5401.098	-2.536	6	1.082	3	90.361	27.137	2	2	4
1B	579.082	5	5.5	2.441	-3.655	19.801	-1.129	53.139	-6.398	8	0.212	2	51.488	114.85	1	-2	4
1C	547.083	3	4	3.901	-4.723	133.618	-0.27	369.961	-4.669	6	0.627	3	74.877	70.32	1	0	4
1D	762.872	1	4.5	5.368	-6.98	51.3	-0.499	571.086	-5.706	6	1.219	1	63.066	115.49	2	1	4
1E	575.137	1	4	5.768	-6.14	1412.911	0.737	4434.814	-2.696	6	1.118	3	91.182	44.124	2	2	4
1F	695.242	1	7	6.37	-6.279	2236.94	0.728	8083.607	-2.495	10	1.14	1	100	63.275	2	2	4
1G	605.08	1	4.5	4.031	-5.499	22.465	-1.025	62.48	-6.414	6	0.931	2	61.776	114.32	1	-2	4
1H	612.028	1	2.5	6.949	-7.752	1477.142	1.116	10000	-3.057	6	1.611	1	100	26.524	2	2	4
1I	571.192	1	2.5	6.518	-6.945	1497.214	0.863	4047.351	-2.999	10	1.599	1	96.027	27.104	2	2	4
1J	680.918	1	2.5	7.385	-7.999	1470.49	1.254	10000	-3.24	6	1.742	1	100	26.535	2	2	4

Table 1: Qikprop results of the compound:

2.5 : Binding free energy:
Molecular docking's most important phase is calculating binding energy to fit a ligand in a binding site. It is usual practice to compute the binding affinities and scoring functions of ligands utilizing binding software such as Gold [37] and Auto Dock [38]. Descriptor-based QSAR models augment the concept of virtual screening and are often very useful in predicting the biological activities of drugs. [39,40] The constantly expanding knowledge of protein libraries combined with virtual screening methodologies based on molecular descriptors facilitates the identification of lead compounds, hence augmenting the entire drug development process. In order to calculate the binding free energy, one must subtract the total free energies of the protein and ligand from the difference in free energies within the complex.
$\Delta G(\text{binding}) = \Delta G(\text{complex}) - \Delta G(\text{protein}) - \Delta G(\text{ligand})$

While the symbols G (complex), G (protein), and G (ligand) represent the free energies of the complex, ligand, and binding, respectively, G (binding) represents the binding free energy.

2.6 Molecular dynamics simulation:

Knowing how simple and macromolecular structures interact at the atomic level is a challenging task for a molecular biologist. The Desmond program [23] was utilized to examine molecular interactions at different time scales. Protein-ligand combinations that scored highest in the virtual screening were selected based on their Glide score. SPC water model was used to store protein-ligand complexes, and box sizes of X = 10, Y = 10, and Z = 10 were specified for the orthorhombic water border box. Counter ions were added to the complex to bring the solvated system into equilibrium. We reduced the complex energy using an OPLS3e force field [24, 25]. It was decided to use a molecular dynamics simulation run length of 100 ns, a recording interval of 100 ps, and an energy of 1.2 ps. The complexes' RMSD and RMSF were investigated following the molecular dynamics run using Maestro's integrated simulation interaction diagram panel. Desmond, a component of Schrodinger's Bio suite, was utilized to investigate the stability of a few docked complexes that were discovered using XP analysis by running molecular dynamics simulations on them [26–28]. These complexes consist of the protein component of the 2VCI (4,5-diarylisooxazole HSP90 chaperone inhibitors) complex and 6-bromo-5-(1,2-dibromo-2-phenylethyl)-7-phenyl-2,3,6,7-tetrahydro-1H-1,4-diazepine.

2.7 Density Functional Theory(DFT):

The density functional theory (DFT) computations were carried out on the synthesized bromo [1,4] benzodiazepine derivatives (1a–1j). All calculations were performed using ORCA 4.2.1 at the B3LYP/def2-SVP level of theory. The current work concentrates primarily on the estimation of different molecular characteristics and reactivity descriptors using the energies of frontier molecular orbitals. [29,30]. To evaluate the reactivity of the compounds, the highest occupied molecular orbital (HOMO) energy, lowest unoccupied molecular orbital (LUMO) energy, and energy gap between the HOMO and LUMO were calculated. [31] These values aid in estimating the reactivity order of the produced compounds (1a–j). The HOMO energy of a molecule represents its capacity to donate electrons. The LUMO energy, on the other hand, indicates the electron-accepting capability of the system. [32,33]. Greater reactivity and the possibility of chemical interactions with biological molecule targets are often indicated by a narrower HOMO-LUMO gap. [34,35] There was a propensity to gain or lose electrons, according on the predicted ionization potential and electron affinity. Nonetheless, their stability and capacity to attract electrons are reflected in their electronegativity and chemical hardness. The ability of a molecule to conduct electrophilic reactions may be gauged by its electrophilicity. The reactivity patterns of these substances in diverse chemical processes were clarified with the help of these descriptors.

3 Results:

3.1 Protein Data Bank (PDB):

Protein Data Bank (PDB ID: 2VCI) [19] provides the 3D structures of the 4,5 Diaryl Isoxazole Hsp90 Chaperone Inhibitors: Potential Therapeutic Agents for Cancer. [36]

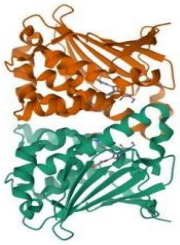

Figure 1:4,5 Diaryl Isoxazole Hsp90 Chaperone Inhibitors(PDB ID:2VCI)

3.2 Molecular Docking Investigation:

Utilizing XP docking, the chosen medication was docked with the target protein, 4,5-Diaryl Isoxazole Hsp90 Chaperone Inhibitors (2VCI). Ten bromo [1,4] benzodiazepine derivative compounds were also put through XP docking. The top three compounds among the bromodiazepine derivatives varied in their top three dock scores and positions, according to the data. 4-(6-bromo-5-(1,2-dibromo-2-(3,4-dihydroxyphenyl) ethyl) -2,3,6,7-tetrahydro-1H-1,4-diazepin-7-yl) benzene-1,2-diol was the most highly rated substance. Compound 1B, with a dock score of -5.9 kcal/mol, established two hydrogen bonds with Asp 54 and Lys 58 (2). 3-bromo-6-bromo-5-(1,2-dibromo-2-(2,3,4-trimethoxyphenyl)ethyl)-7-(2,3,4 trimethoxyphenyl) -2,3,6,7-tetrahydro-1H-1,4-diazepine was the second-placed chemical with a docking score of -5.2 kcal/mol, but it had no interaction. 4-(6-bromo-5-(1,2-dibromo-2-(4hydroxyphenyl) ethyl) -2,3,6,7-tetrahydro-1H-1,4-diazepin-7-yl) phenol had a docking score of -5.0 kcal/mol and established three hydrogen bonds with Leu 48, Ser 52, and Gly 108. With

a dock score of -6.0 kcal/mol, the commonly used medication, Binimetinib, formed three hydrogen bonds with the residues Lys 58, Gly 07, and Leu 107 during its contact with these three residues. The targeted protein interacted with nine of the 10 diazepine derivatives, whereas no interaction was seen with the 1F drug.

Figure 2: Molecular docking of Structures of 1A to 1J and its Standard drug

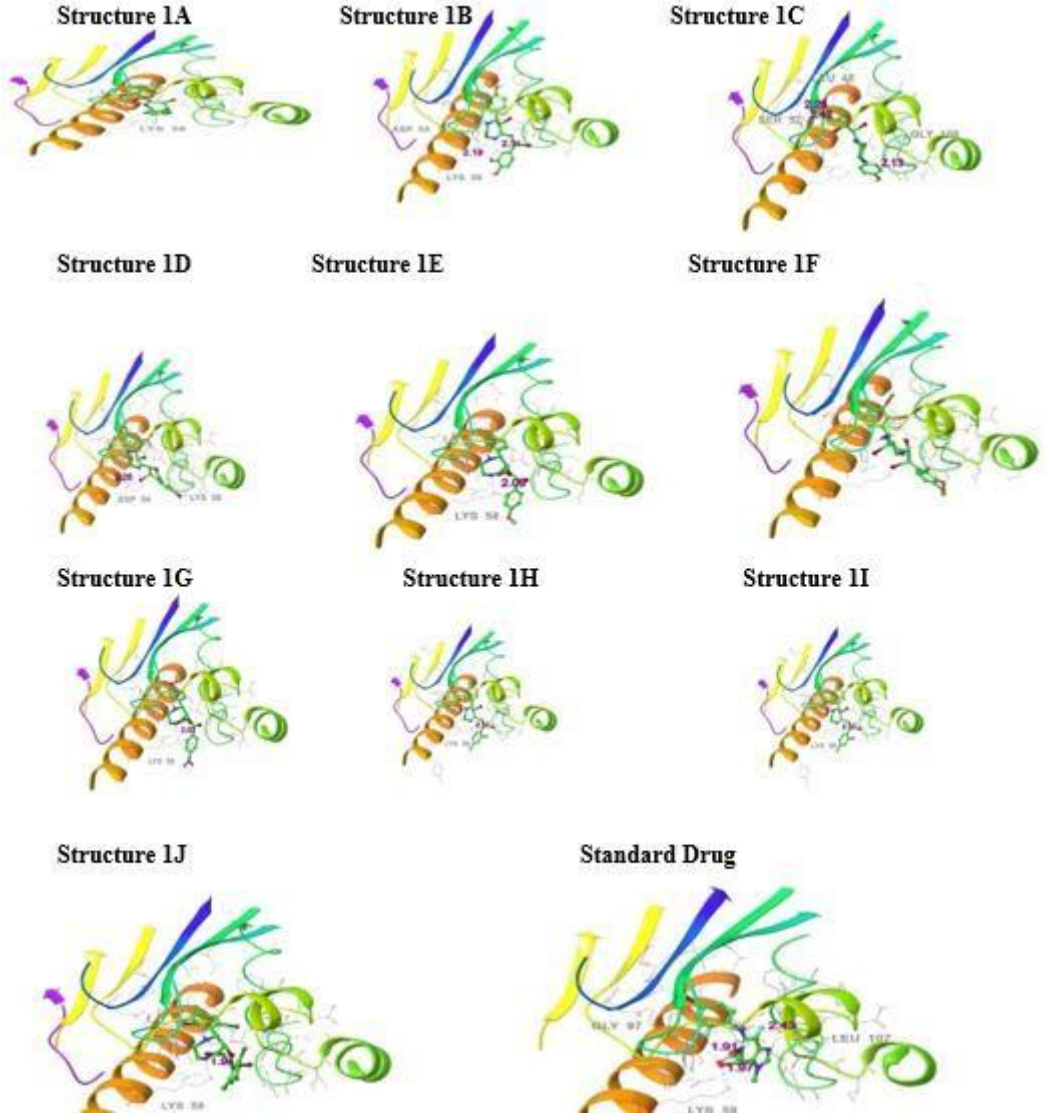

Table 2: XP Docking Results of the compounds:

S.No	Compound Name	Dock Score	No of residues	Interacting residues	Bond Length
1.	Structure 1B	-5.9	3	Asp 54, Lys 58(2)	2.19, 2.31, 3.60
2.	Structure 1F	-5.2	-	-	-
3.	Structure 1C	-5.0	3	Leu 48, Ser 52, Gly 108	2.42, 2.25, 2.13
4.	Structure 1I	-4.9	1	Lys 58	1.92
5.	Structure 1D	-4.5	2	Asp 54 (salt bridge), Lys 58	4.17, 2.25
6.	Structure 1A	-4.4	1	Lys 58	3.11
7.	Structure 1H	-4.2	1	Lys 58	2.37
8.	Structure 1E	-3.7	2	Lys 58(2) (Pi-cation)	2.09, 3.07
9.	Structure 1G	-3.5	3	Lys 58(3) (Pi-cation, Salt bridge)	2.03, 3.24, 4.56
10.	Structure 1J	-2.6	1	Lys 58	1.94
11.	Standard drug	-6.0	3	Lys 58, Gly 07, Leu 107	1.97, 1.91, 2.43

3.3 Binding free energy calculation:

Table 3 can be used to compute the target-ligand complexes' free energies. In this instance, the stronger the connection, the larger the negative number. It was determined that the medication's binding affinity was -37.21. Structure 1B's binding affinity was higher than that of a typical drug. In our investigation, Structure 1I's exhibits free energy values that are quite low compared to other target-ligand complexes. The bulk of the chemicals typically have a rather high binding affinity. The reference ligand value and the free energy value of Structure 6 are the most similar.

Table 3: Binding free energy calculations of the compound

S.No	Compound	MMGBSA dG Bind
1.	**Structure 1B**	-41.95
2.	**Structure 1F**	-32.61
3.	**Structure 1C**	-21.45
4.	**Structure 1I**	-11.58
5.	**Structure 1D**	-16.83
6.	**Structure 1A**	-14.67
7.	**Structure 1H**	-27.79
8.	**Structure 1E**	-27.73
9.	**Structure 1G**	-28.10
10.	**Structure 1J**	-21.74
11	**Standard Drug**	**-37.21**

3.4 Molecular dynamic simulation:

3.4.1 RMSD analysis:

During dynamics analysis, the stability of the protein-ligand complex was ascertained using the RMSD values of the protein backbone, as seen in Fig 3. By employing a complex docked structure with 4-(6-bromo-5-(1,2-dibromo-2-(3,4-dihydroxy phenyl)ethyl)-2,3,6,7-tetrahydro-1H-1,4-diazepine-7-yl)benzene-1,2-diol, the stability of the 4,5-Diaryl Isoxazole Hsp90 Chaperone Inhibitors Component was assessed.

Figure 3: RMSD plotof the Docked complex structure of 4,5-Diaryl Isooxazole Hsp90 Chaperone with 4-(6-bromo-5-(1,2-dibromo-2-(3,4-dihydroxyphenyl)ethyl)-2,3,6,7- tetrahydro-1H-1,4-diazepin-7-yl)benzene-1,2-diol.

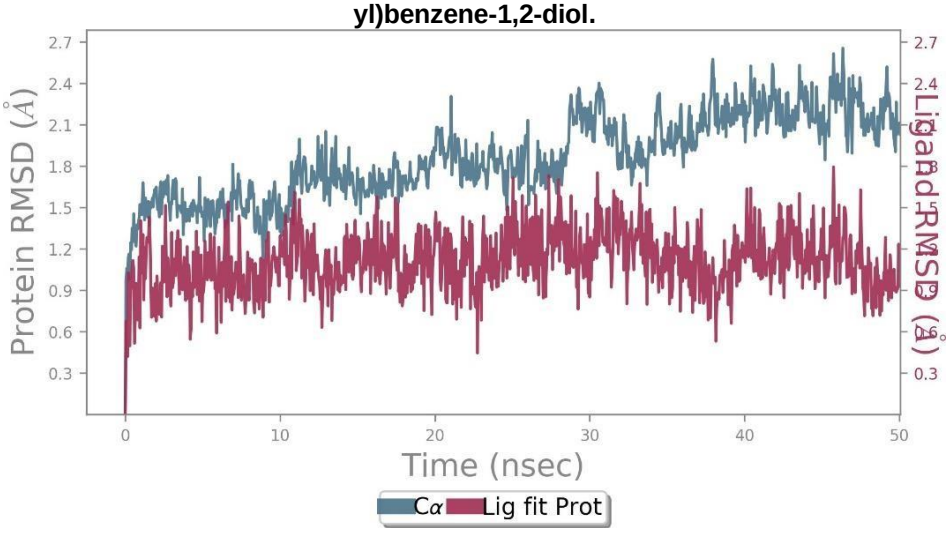

3.4.2 RMSF Analysis:

The compound showed stability between 0 to 50 ns, with fluctuations in the protein's C alpha atoms and heavy ligand atoms within a 3Å range. This implies a robust connection between the protein and ligand, enhancing the complex's stability. [41]

Figure 4: RMSD plotof the Docked complex structure of 4,5-Diaryl Isooxazole Hsp90 Chaperone with 4-(6-bromo-5-(1,2-dibromo-2-(3,4-dihydroxyphenyl)ethyl)-2,3,6,7- tetrahydro-1H-1,4-diazepin-7-yl)benzene-1,2-diol.

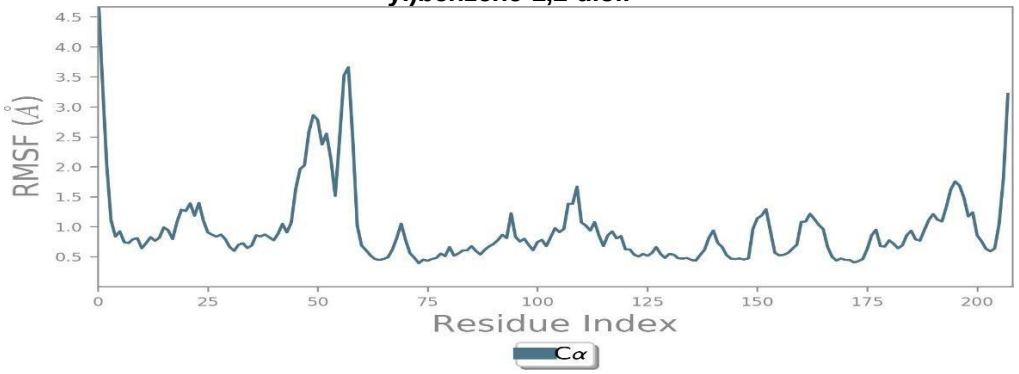

3.4.3 Protein-ligand interactions:

There are four types of interactions that proteins and their ligands can have: hydrogen bonds, hydrophobic bonds, water bridges, and ionic bonds. Hydrogen bonds, in particular, are important in pharmaceutical design because they impact medication selectivity, metabolism, and absorption. [42,43] A prominent hydrogen bond was observed between the ligand and key residues in the complex structure of 4,5-Diaryl Isoxazole Hsp90 Chaperone Inhibitors with 4-(6-bromo-5-(1,2-dibromo-2-(3,4-di hydroxyphenyl) ethyl). -2,3,6,7-tetrahydro-1H-1,4-diazepin-7-yl) benzene-1,2-diol. This indicates a strong interaction at the binding site. ASN 51, SER 52, ASP 93, GLY 97, GLY 135, and THR 184 were all implicated in hydrogen interactions. ASN 51, ASP 54, LUS 58, ASN 106, THR 109, ILE 110, ALA 111, GLY 135, GLY 137, and TYR 139 also created water bridges, whereas ALA 55, MET 98, LEU 107, and PHE 138 established hydrophobic connections. (Ref Figure:11) According to the timeline depiction (Figure 6 below), the residues are ASN 51, ALA 55, ASP 93, GLY 97, and GLY 135. PHE 138, THR 184, and others maintained the connections for the longest feasible duration during the experiment.

The contacts between the residues ASP 93, GLY 97, THR 184, GLY 135, ASN 51, TYR 139, and THR 109 were maintained in proportions of 100%, 77%, 55%, 34%, 37%, 55%, and 58% across the simulation duration, respectively, according to the 2D depiction of the complexed structure. Figure 11 shows the interaction of 4,5-Diaryl Isoxazole Hsp90 Chaperone Inhibitors with 4-(6-bromo-5-(1,2-dibromo-2-(3,4-dihydroxy phenyl) ethyl). -2,3,6,7-tetrahydro-1H-1,4-diazepin-7-yl) benzene-1,2-diol (Ref. Figure 7)

The compound produced by 4-(6-bromo-5-(1,2-dibromo-2-(3,4-dihydroxyphenyl) ethyl)-2,3,6,7-tetrahydro-1H-1,4-diazepin-7-yl) benzene-1,2-diol and 4,5-Diaryl Isoxazole Hsp90 Chaperone was stable, based upon the results of the Molecular Dynamics simulation research. In the XP study, it demonstrated significant interactions with the functionally conserved residues ASP 93 and GLY 97, as well as the interacting residues ASP 54 and LYS 58(2). This simulation study suggests that 4-(6-bromo-5-(1,2-dibromo-2-(3,4-dihydroxyphenyl) ethyl)-2,3,6,7-tetrahydro-1H-1,4-diazepin-7-yl) benzene-1,2-diol could possess anticancer properties with 4,5-Diaryl Isoxazole Hsp90 Chaperone.

Figure 5:Graph illustrating the interaction between protein and ligands in a Docked complex structure of 4,5-Diaryl Isooxazole Hsp90 Chaperone with 4-(6-bromo-5-(1,2-dibromo-2-(3,4-dihydroxyphenyl)ethyl)-2,3,6,7- tetrahydro-1H-1,4-diazepin-7-yl)benzene-1,2-diol.

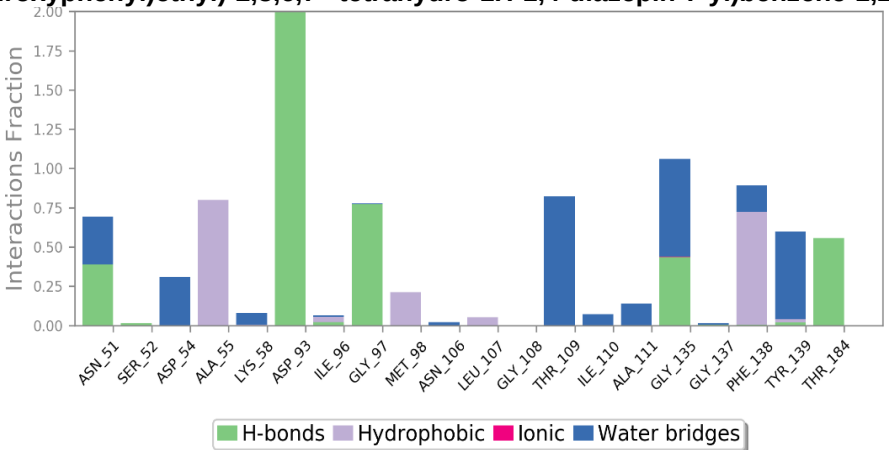

Figure 6: Time line representation of complex structure of 4,5-Diaryl Isooxazole Hsp90 Chaperone with 4-(6-bromo-5-(1,2-dibromo-2-(3,4-dihydroxyphenyl)ethyl)-2,3,6,7- tetrahydro-1H-1,4-diazepin-7-yl)benzene-1,2-diol.

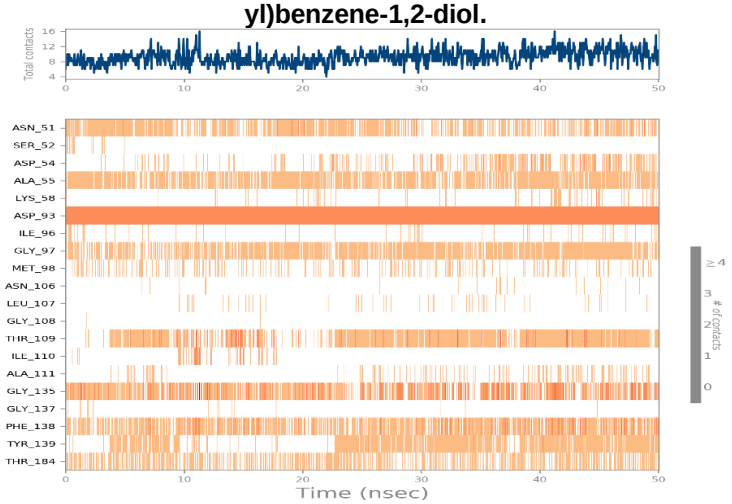

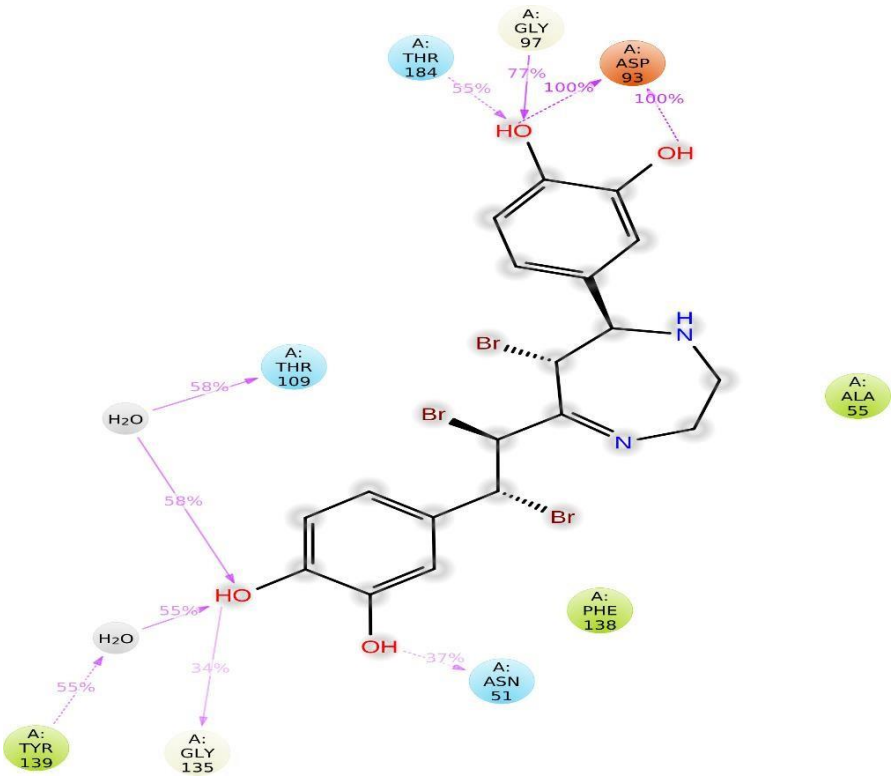

Figure 7: 2D structure of interaction of 4,5-Diaryl Isooxazole Hsp90 Chaperone with 4-(6-bromo-5-(1,2-dibromo-2-(3,4-dihydroxyphenyl)ethyl)-2,3,6,7- tetrahydro-1H-1,4-diazepin-7-yl)benzene-1,2-diol.

3.4.4 Molecular electrostatic potential surface:

Figure:8 Optimized Structures of compound 4-(6-bromo-5-(1,2-dibromo-2-(3,4-dihydroxyphenyl)ethyl)-2,3,6,7- tetrahydro-1H-1,4-diazepin-7-yl)benzene-1,2-diol showing electrostatic potential surface

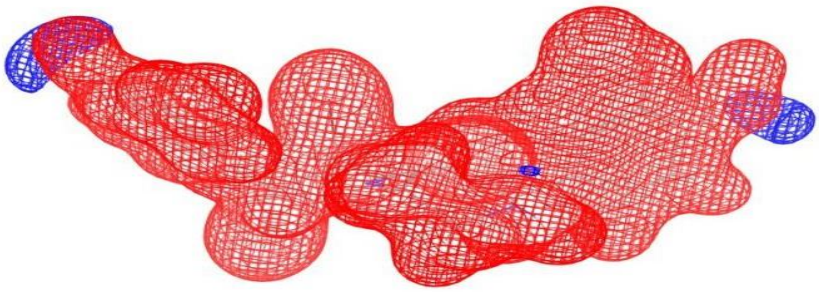

To analyze the compound of 4-(6-bromo-5-(1,2-dibromo-2-(3,4-dihydroxy phenyl) ethyl)-2,3,6,7-tetrahydro-1H-1,4-diazepin-7-yl) benzene-1,2-diol, non-bonding interactions between molecules, and to anticipate the reactivity characteristics of molecular systems, such as the identification of probable electrophilic and nucleophilic reaction sites, the electrostatic potential (ESP) surface is a potent descriptor The MEP surface analysis of the molecule was computed by the DFT calculation using the optimized structure and the B3LYP/6-31G(d,p) basis set. The chemical under investigation's mapped electrostatic potential surface is displayed in Fig. 8. The red and blue hues of the MEP structure represent more electron-rich and electron-poor areas, respectively. There is a discernible polarization effect to the chemical. The electropositive atoms (hydrogen) are localized over the positive potential regions in the MEP, whereas the electronegative atoms (oxygen, nitrogen, and sulfur) are concentrated over the negative potential areas. The sulfur atom does, however, have a less negative potential location than the other electronegative atoms in the molecule. Consequently, locations with more positive electrostatic potential and greater negative electronegative potential tend to attract more nucleophilic and electrophilic organisms.

3.4.5 Electrostatic results and Mullikan electronegativity:

A molecule's ability to donate and receive electrons may be ascertained using its HOMO and LUMO energy levels. These molecular orbitals are important for understanding biological mechanisms, luminescence,

photochemical processes, electrical and optical properties, UV-VIS, quantum chemistry, and pharmaceutical research [44–49]. Structural stability is demonstrated by the energy gap of the frontier molecular orbital, or FMO. The chemical reactivity and kinetic stability of a molecule are further characteristics revealed by FMOs. Additionally, the FMOs help predict the most reactive region of a chemical under investigation. The 4-(6-bromo-5-(1,2-dibromo-2-(3,4-dihydroxy phenyl) ethyl)-2,3,6,7-tetrahydro-1H-1,4-diazepin-7-yl) benzene-1,2-diol anticipated energy orbitals for the HOMO and LUMO-0.24 and -0.078 eV, respectively.It was found that the aforementioned organic molecule had an energy gap of 0.16 eV between its ($\Delta E_{HOMO-LUMO}$) FMOs. The analyzed molecule displays strong chemical reactivity, biological activity, and polarizability, as evidenced by the decreased HOMO and LUMO energy gaps. The compound's FMO distribution is shown in Figure 9.

Figure 9: HOMO and LUMO of the compound 4-(6-bromo-5-(1,2-dibromo-2-(3,4-dihydroxyphenyl) ethyl)-2,3,6,7- tetrahydro-1H-1,4-diazepin-7-yl) benzene-1,2-diol.

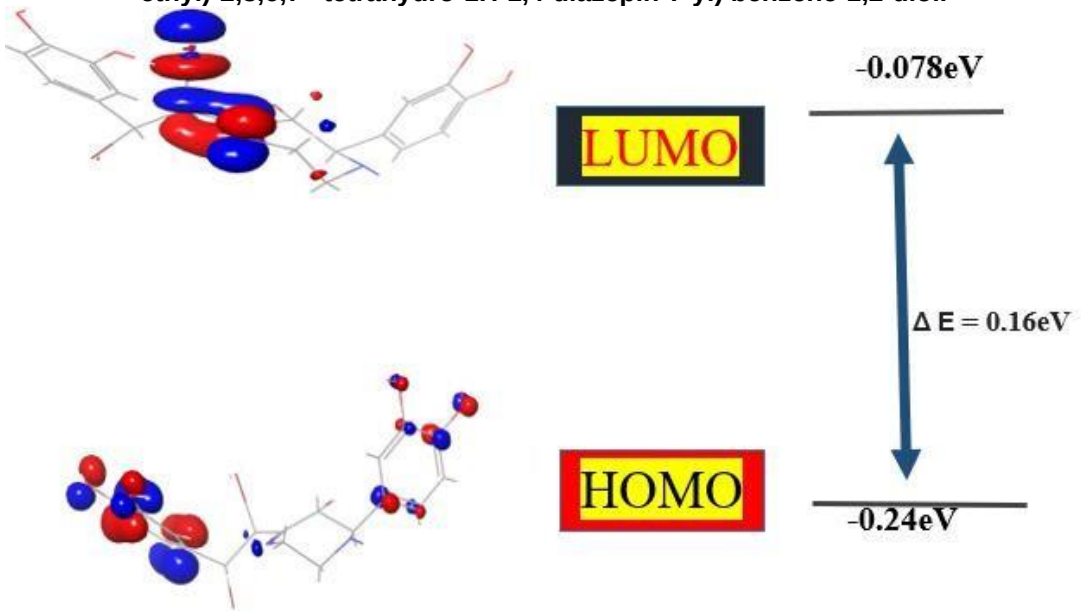

The computed values for the assessed molecule's chemical potential, chemical hardness, electrophilicity index, and chemical softness were 0.08, -0.15, 0.15 eV, and 12.2 eV-1, in that order. An indicator of a compound's capacity to attach to biomolecules is its electrophilicity index [50–52]. The greater the molecule's electrophilicity index value, the more electrophilic a species it may become and the greater its ability to bind biomolecules. A lower chemical hardness value and a larger negative chemical potential value imply that the chemical under investigation is soft and polarizable. Furthermore, partial detections of HOMO orbitals have been made on the nitrogen atoms (N20, N23), a phenyl ring that is joined by four hydroxygen groups, and mostly on the oxygen atoms (O25, O26, O27, and O28). (Fig. 9).

4. Conclusion:

By using molecular docking, the developed derivative's binding potential was hypothesized. The 1B molecule was found being the most effective against skin cancer by molecular docking analyses of all 10 molecules. Following that, MD simulations and DFT were used to verify and validate the precision and correctness of binding with the 4,5-diaryl isoxazole Hsp90 chaperone inhibitors. The suggested compound displays excellent stability in the active site of 4,5-diaryl isoxazole Hsp90 Chaperone, according to MD simulations. To evaluate the ligand-protein complex's stability, RMSD, and RMSF values, MD simulation was performed.The estimated DFT characteristics demonstrate that the substance is chemically reactive. Additionally, the drug-likeness was revealed by ADMET assays. According to the material, these results encourage further in vitro and in vivo anticancer research.

References:

1. An S, Kim K, Moon S, Ko KP, Kim I, Lee JE, et al. Inanotechnology-empowered strategies in treatment of skin cancer. Environ ancer: Systematic review and meta-analysis. Cancers (Basel). 2021; 13:5940 MDPI.
2. Chandra J, Hasan N, Nasir N, Wahab S, Thanikachalama PV, Sahebkar A, et al. Nanotechnology-empowered strategies in treatment of skin cancer. Environ Res. 2023;235:116649.Availablefrom: https://linkinghub.elsevier.com/retrieve/pii/S0013935123014536. Cited 2023 Jul 17. Academic Press.

3. Hasan N, Imran M, Sheikh A, Tiwari N, Jaimini A, Kesharwani P, et al. Advanced multifunctional nano-lipid carrier loaded gel for targeted delivery of 5-flurouracil and cannabidiol against non-melanoma skin cancer. Environ Res. 2023; 233:116454. Available from: https://linkinghub.elsevier.com/retrieve/pii/S0013935123012586. Cited 2023 Jul 2. Academic Press.
4. Hasan, N., Nadaf, A., Imran, M. *et al.* Skin cancer: understanding the journey of transformation from conventional to advanced treatment approaches. *Mol Cancer* 22, 168 (2023). https://doi.org/10.1186/s12943-023-01854-3
5. Rogers HW, Weinstock MA, Feldman SR, Coldiron BM. Incidence Estimate of Nonmelanoma Skin Cancer (Keratinocyte Carcinomas) in the U.S. Population, 2012. JAMA Dermatol. 2015 Oct;151(10):1081-6. [PubMed]
6. Glazer AM, Winkelmann RR, Farberg AS, Rigel DS. Analysis of Trends in US Melanoma Incidence and Mortality. JAMA Dermatol. 2017 Feb 01;153(2):225-226. [PubMed]
7. The Global Cancer Observatory, Cancer Today, 2020. [(accessed on 1 February 2021)]. Available online: https://gco.iarc.fr/today/fact-sheets-cancers
8. World Cancer Research Fund International Skin Cancer Statistics. [(accessed on 1 February 2021)]. Available online: https://www.wcrf.org/dietandcancer/cancer-trends/skin-cancer-statistics
9. Guan L., Yang H., Cai Y., Sun L., Di P., Li W., Liu G., Tang Y. ADMET-score–a comprehensive scoring function for evaluation of chemical drug-likeness. *Med. Chem. Comm.* 2019; 10:148–157. doi: 10.1039/C8MD00472B. [PMC free article] [PubMed] [CrossRef] [Google Scholar]
10. 28. Vardhan S., Sahoo S.K. In silico ADMET and molecular docking study on searching potential inhibitors from limonoids and triterpenoids for COVID-19. *Comput. Biol. Med.* 2020; 124:103936. doi: 10.1016/j.compbiomed.2020.103936. [PMC free article] [PubMed] [CrossRef] [Google Scholar]
11. 29. Chen G., Seukep A., Guo M. Recent advances in molecular docking for the research and discovery of potential marine drugs. *Mar. Drugs.* 2020; 18:545. doi: 10.3390/md18110545. [PMC free article] [PubMed] [CrossRef] [Google Scholar]
12. Recent Development in[1,4]Benzodiazepines as Potent Anticancer Agents: A Review Author(s): Rupinder Kaur Gill, Shiv Om Kaushik, Jasreen Chugh, Sumit Bansal, Anamik Shah and Jitender Bariwal Volume 14, Issue 3, 2014Page: [229 - 256]Pages: 28 DOI: 10.2174/13895575113139990081
13. Byrd A.L., Belkaid Y., Segre J.A. The Human Skin Microbiome. *Nat. Rev. Microbiol.* 2018; 16:143–155. doi: 10.1038/nrmicro.2017.157. [PubMed] [CrossRef] [Google Scholar]
14. Morris, G.M., Lim-Wilby, M. (2008). Molecular Docking. In: Kukol, A. (eds) Molecular Modeling of Proteins. Methods Molecular Biology™, vol 443. Humana Press. https://doi.org/10.1007/978-1-59745-177-2_19
15. D. Plewczynski, M. Lazniewski, R. Augustyniak, K. Ginalski, J. Comput. Chem. 32 (2011) 742.
16. R.D. Smith, J.B. Dunbar Jr., P.M. Ung, E.X. Esposito, C.Y. Yang, S. Wang, H.A. Carlson, J. Chem. Inf. Model 51 (2011) 2115.
17. Z. Gaieb, S. Liu, S. Gathiaka, M. Chiu, H. Yang, C. Shao, V.A. Feher, W.P. Walters, B. Kuhn, M.G. Rudolph, S.K. Burley, M.K. Gilson, R.E. Amaro, J Comput. Aided Mol. Des. 32 (2018) 1.
18. N.S. Pagadala, K. Syed, T.J, Biophys. Rev. 9 (2017) 91
19. RCSB, P. The Research Collaboratory for Structural Bioinformatics Protein Data Bank. 2014. Available online: http://www.rcsb. org/pdb (accessed on 1 May 2022).
20. Dong J, Wang N-N, Yao Z-J, Zhang L, Cheng Y, Ouyang D, Ai-Ping Lu, Cao D-S. ADMET lab: a platform for systematic ADMET evaluation based on a comprehensively collected ADMET database. *J Cheminform.* 2018;10(1):29. doi: 10.1186/s13321-018-0283-x. [PMC free article] [PubMed] [CrossRef] [Google Scholar]
21. Teli MK, Rajanikant GK. Identifications of novel potential HIF-prolyl hydroxylase inhibitors by in silico screening. *Mol Divers.* 2012;16(1):193–22. doi: 10.1007/s11030-011-9338-x. [PubMed] [CrossRef] [Google Scholar]
22. Salmas RE, Unlu A, Bektaş M, Yurtsever M, Mestanoglu M, Durdagi S. Virtual screening of small molecules databases for the discovery of novel PARP-1 inhibitors: a combination of in silico and in vitro studies. *J Biomol Struct Dyn.* 2017;35(9):1899–1915. doi: 10.1080/07391102.2016.1199328. [PubMed] [CrossRef] [Google Scholar]
23. Vijayakumar S, Manogar P, Prabhu S, Singh RASK. Novel ligand-based docking; molecular dynamic simulations; and absorption, distribution, metabolism, and excretion approach to analyzing potential Acetylcholinesterase inhibitors for Alzheimer's disease. *J Pharm Anal.* 2018;8(6):413–420. doi: 10.1016/j.jpha.2017.07.006. [PMC free article] [PubMed] [CrossRef] [Google Scholar]
24. F. Bracht and R. B. de Alencastro, *J. Biomol. Struct. Dyn.*, 2016, 34(2), 259– 271
25. Docking studies and molecular dynamics simulation of triazole benzene sulfonamide derivatives with human carbonic anhydrase IX inhibition activity P and Kathiravan M.K.* *Dr. A. P. J. Abdul Kalam Research Lab, Department of Pharmaceutical Chemistry, SRM College of Pharmacy, SRMIST, Kattankulathur,* DOI: 10.1039/D1RA07377J
26. R. Haunschild, A. Barth, B. French, A comprehensive analysis of the history of DFT based on the bibliometric method RPYS, J. Cheminf. 11 (2019) 1e15.
27. X. Ma, D. Chang, C. Zhao, R. Li, X. Huang, Z. Zeng, X. Huang, Y. Jia, Geometric structures and electronic properties of the Bi2X2Y (X, Y¼O, S, Se, and Te) ternary compound family: a systematic DFT study, J. Mater. Chem. 6 (2018) 13241e13249.18

28. S. Naseem, M. Khalid, M.N. Tahir, M.A. Halim, A.A.C. Braga, M.M. Naseer, Z. Shafiq, Synthesis, structural, DFT studies, docking and antibacterial activity of a xanthene based hydrazone ligand, J. Mol. Struct. 1143 (2017) 235e244.
29. Kilbile, J. T.; Tamboli, Y.; Ansari, S. A.; Rathod, S. S.; Choudhari, P. B.; Alkahtani, H.; Sapkal, S. B. Synthesis, Biological Evaluation, and Computational Studies of 6-Fluoro-3-(Piperidin-4-Yl)-1,2-Benzisoxazole Sulfonamide Conjugates. *Polycyclic Aromat. Compd.* 2023, 1– 21, DOI: 10.1080/10406638.2023.224711
30. Bakale, R. D.; Sulakhe, S. M.; Kasare, S. L.; Sathe, B. P.; Rathod, S. S.; Choudhari, P. B.; Madhu Rekha, E.; Sriram, D.; Haval, K. P. Design, Synthesis and Antitubercular Assessment of 1, 2, 3-Triazole Incorporated Thiazolylcarboxylate Derivatives. *Bioorg. Med. Chem. Lett.* 2024, *97*, 129551, DOI: 10.1016/j.bmcl.2023.129551
31. Rathod, S.; Bhande, D.; Pawar, S.; Gumphalwad, K.; Choudhari, P.; More, H. Identification of Potential Hits against Fungal Lysine Deacetylase Rpd3 via Molecular Docking, Molecular Dynamics Simulation, DFT, In-Silico ADMET and Drug-Likeness Assessment. *Chem. Afr.* 2024, *7*, 1151– 1164, DOI: 10.1007/s42250-023-00766-5
32. Choudhari, S.; Patil, S. K.; Rathod, S. Identification of Hits as Anti-Obesity Agents against Human Pancreatic Lipase via Docking, Drug-Likeness, in-Silico ADME(T), Pharmacophore, DFT, Molecular Dynamics, and MM/PB(GB)SA Analysis. *J. Biomol. Struct. Dyn.* 2023, 1– 23, DOI: 10.1080/07391102.2023.2258407
33. Rochlani, S.; Bhatia, M.; Rathod, S.; Choudhari, P.; Dhavale, R. Exploration of Limonoids for Their Broad Spectrum Antiviral Potential via DFT, Molecular Docking and Molecular Dynamics Simulation Approach. *Nat. Prod. Res.* 2023, *38*, 891– 896, DOI: 10.1080/14786419.2023.2202398
34. Patial, P. K.; Cannoo, D. S. Phytochemical Profile, Antioxidant Potential and DFT Study of Araucaria Columnaris (G. Forst.) Hook. Branch Extracts. *Nat. Prod. Res.* 2021, *35* (22), 4611– 4615, DOI: 10.1080/14786419.2019.1696330
35. Amer, M. M. K.; Abdellattif, M. H.; Mouneir, S. M.; Zordok, W. A.; Shehab, W. S. Synthesis, DFT Calculation, Pharmacological Evaluation, and Catalytic Application in the Synthesis of Diverse Pyrano[2,3-c]Pyrazole Derivatives. *Bioorg. Chem.* 2021, *114*, 105136, DOI: 10.1016/j.bioorg.2021.105136
36. 4,5 Diaryl Isoxazole Hsp90 Chaperone Inhibitors: Potential Therapeutic Agents for the Treatment of Cancer PDB DOI: https://doi.org/10.2210/pdb2VCI/pdb
37. (ADMET) Hsp90 Inhibitor Geldanamycin Enhances the Antitumor Efficacy of Enediyne Lidamycin in Association with Reduced DNA Damage Repair Fei-Fei Han&, Liang Li&, Bo-Yang Shang, Rong-Guang Shao, Yong-Su Zhen*DOI:http://dx.doi.org/10.7314/APJCP.2014.15.17.7043
38. Jones, G.; Willett, P.; Glen, R.; Leach, A.; Taylor, R., Development and validation of a genetic algorithm for flexible docking. J Mol Biol 1997, 267 (3), 727-748.
39. Morris, G.; Goodsell, D.; Huey, R.; Olson, A., Distributed automated docking of flexible ligands to proteins: parallel applications of AutoDock 2.4. J Comp-Aided Mol Des 1996, 10 (4), 293-304.
40. Anti-Tubercular Drug Designing Using Structural Descriptors Manish C. Bagchi1,* and Payel Ghosh2 1 School of Bioscience & Engineering, Jadavpur University, Kolkata 700032, India and 2 Department of Biotechnology, University of Pune, Pune-411007, India
41. Finding new inhibitors for EML4-ALK fusion protein: a computational approach K Sabitha, R Vijayalakshmi - 2012 - International Research Journal of Pharmacy
42. Prediction of Protein-Ligand Binding Poses via a Combination of Induced Fit Docking and Metadynamics Simulations Anthony J. Clark, Pratyush Tiwary, Ken Borrelli, Shulu Feng, Edward B. Miller, Robert Abel, Richard A. Friesner , and B. J. Berne
43. Screening Balanites aegyptiaca for inhibitors against putative drug targets in Microsporum gypseum – Subtractive proteome, docking and simulation approach Mohamed Hussain Syed Abuthakir, Velusamy Sharmila, Muthusamy Jeyam https://doi.org/10.1016/j.meegid.2021.104755.
44. H. Ebrahimi, J.S. Hadi, H.S. Al-Ansari, A new series of Schiff bases derived from sulfa drugs and indole-3-carboxaldehyde: synthesis, characterization, spectral and DFT computational studies, J. Mol. Struct. 1039 (2013) 37e45.
45. S.A. Beyramabadi, Fluorescence and DFT studies (molecular structure, IR and NMR spectral assignments, NBO and Fukui function) of Schiff bases derived from 2-chloro-3-quinolinecarboxaldehyde, J. Struct. Chem. 59 (2018) 1392e1402.
46. H.P. Ebrahimi, J.S. Hadi, A.A. Almayah, Z. Bolandnazar, A.G. Swadi, A. Ebrahimi, Metal-based Biologically Active Azoles and b-lactams Derived from Sulfa Drugs, Elsevier Ltd, 2016.
47. Z. Demircioglu, Ç.A. Kas ¸ tas¸, O. Büyükgüngor, The spectroscopic (FT-IR, UV-vis), € fukui function, NLO, NBO, NPA and tautomerism effect analysis of (E)-2- [(2- hydroxy-6-methoxybenzyli- dene) amino] benzonitrile, Spectrochim. Acta Mol. Biomol. Spectrosc. 139 (2015) 539e548.
48. S. Kumar, V. Saini, I.K. Maurya, J. Sindhu, M. Kumari, R. Kataria, V. Kumar, Design, synthesis, DFT, docking studies and ADME prediction of some new coumarin linked pyrazolyl thiazoles : potential standalone or adjuvant antimicrobial agents, PloS One 13 (2018) 1e23
49. DFT studies on vibrational and electronic spectra, HOMOeLUMO, MEP, HOMA, NBO and molecular docking analysis of benzyl-3-N-(2,4,5trimethoxyphenylmethylene) hydrazinecarbodithioate Mohammad

Abdul Mumit a, Tarun Kumar Pal a, *, Md Ashraful Alam a, Md Al-Amin-Al-Azadul Islam a, Subrata Paul b, Md Chanmiya Sheikh c

50. S. Alyar, S. Tülin, Synthesis, spectroscopic characterizations, enzyme inhibition, molecular docking study and DFT calculations of new Schiff bases of sulfa drugs, J. Mol. Struct. 1185 (2019) 416e424.
51. S. Mondal, S.M. Mandal, T.K. Mondal, C. Sinha, Structural characterization of new Schiff bases of sulfamethoxazole and sulfathiazole, their antibacterial activity and docking computation with DHPS protein structure, Spectrochim. Acta Mol. Biomol. Spectrosc. 150 (2015) 268e279.
52. G. Banuppriya, R. Sribalan, V. Padmini, Synthesis and characterization of curcumin-sulfonamide hybrids: biological evaluation and molecular docking studies, J. Mol. Struct. 1155 (2018) 90e100.

DOI: https://doi.org/10.15379/ijmst.v10i4.3653